

Journal of Photonics for Energy

SPIDigitalLibrary.org/jpe

High efficiency white organic light emitting diodes employing blue and red platinum emitters

Barry O'Brien
Gregory Norby
Guijie Li
Jian Li

High efficiency white organic light emitting diodes employing blue and red platinum emitters

Barry O'Brien,^{a,b} Gregory Norby,^a Guijie Li,^a and Jian Li^{a,b,*}

^aArizona State University, Department of Material Science, Tempe, Arizona 85284

^bArizona State University, Flexible Display Center, 7700 South River Parkway, Tempe, Arizona 85284

Abstract. Platinum-based blue and red emitters were used to make stacked organic light-emitting diodes devices for potential use in solid-state lighting. The electroluminescence (EL) spectra were strongly dependent on the red layer thickness and relative position of the red and blue emissive layers. Although all devices had very little EL in the green region, a color rendering index (CRI) as high as 65 was achieved. Addition of a suitable phosphorescent green emissive layer should produce higher CRI values. All devices tested exhibited external quantum efficiencies greater than 20%, indicating that the Pt-based emitters reported here are potentially useful for solid-state lighting applications. © 2014 Society of Photo-Optical Instrumentation Engineers (SPIE) [DOI: [10.1117/1.JPE.4.043597](https://doi.org/10.1117/1.JPE.4.043597)]

Keywords: organic light emitting diode; electrophosphorescence; Pt-based emitters; solid-state lighting; photonics.

Paper 13045SS received Dec. 28, 2013; revised manuscript received Mar. 5, 2014; accepted for publication Mar. 6, 2014; published online Apr. 11, 2014.

1 Introduction

Rising worldwide energy demand and limited supply of traditional energy sources have spurred research in alternative energy generation methods and improving energy efficiency for existing applications. Lighting, which by some estimates accounts for 20% of electrical energy consumption, is one major field targeted for improved energy efficiency.¹ In fact, one United States Department of Energy estimate predicts that increased use of solid-state lighting could halve the domestic lighting energy demand by 2030, saving 300 TW h of energy and cutting greenhouse emissions by the equivalent of 40 million cars.² Current lighting sources primarily employ either short lasting, inefficient incandescent bulbs or fluorescent lighting which contain hazardous materials such as mercury that complicates their disposal. Solid-state approaches using inorganic or organic materials are becoming increasingly studied due to their potential to produce light much more efficiently, with longer operational lifetime, while using environmentally benign materials.³ Inorganic lighting sources have reached laboratory power efficiencies greater than 250 Lm/W and have been commercially available since 2008.⁴ However, the cost of these sources remains high and fabrication complexities may prohibit production on a large enough scale to replace all the current incandescent and fluorescent bulbs. Organic lighting sources have been proposed as an alternative solid-state lighting source due to potentially low-cost fabrication processes, the ability to be deposited on a wide array of cheap substrates in a large number of unique form factors, and their ability to be easily color tuned.^{5,6} Furthermore, white organic light emitting diodes (WOLEDs) have demonstrated efficiencies exceeding fluorescent light.⁷ Nevertheless, in order to compete with the efficiency and stability of inorganic solid-state lighting or the cost effectiveness of fluorescent lighting, more work is needed to meet commercial needs.

In order to realize the mass production of WOLEDs for solid-state lighting, stable and efficient emitters are vital to develop. A large number of efficient red, green, and blue OLEDs have

*Address all correspondence to: Jian Li, E-mail: jian.li.1@asu.edu

been reported based on phosphorescent complexes due to their ability to harvest 100% of electro-generated excitons.^{8,9} However, the development of stable and efficient white devices remains a challenge.¹⁰ Most of the phosphorescent emitters for WOLEDs have focused on Ir-based compounds due to their high efficiencies, well-studied photophysical properties and demonstrated stability across a large range of the visible spectrum.^{11,12} Recently, platinum-based emitters have demonstrated efficiencies that are similar or superior to their iridium analogs, yet Pt complexes remain less researched than Ir compounds.^{13–15} This article investigates the development of Pt compounds as red–orange and blue emitters for application to solid-state lighting.

2 Experiment Result

2.1 Materials

Dipyrazino[2,3-f:2',3'-h]quinoxaline- 2,3,6,7,10,11-hexacarbonitrile (HATCN) was obtained from Lumtec and N,N'-Bis(naphthalen-1-yl)-N,N'-bis(phenyl)-benzidine (NPD) was obtained from Chemical Alta. Di-[4-(N,N-ditolyl-amino)-phenyl]cyclohexane (TAPC),¹⁶ 2,6-bis(N-carbazolyl) pyridine (26mCPy),¹⁷ diphenylbis(4-(pyridine-3-yl)phenyl)silane (DPSS),¹⁸ 1,3-bis(3,5-dipyrid-3-yl-phenyl)benzene (BmPyPB),¹⁹ and PtON1 (shown in Fig. 1)²⁰ were prepared following the previous literature procedures. All organic materials were sublimed in a thermal gradient furnace prior to use.

2.2 PtN3N-ptb Synthesis

Synthesis of PtN3N-ptb: To a dry pressure tube equipped with a magnetic stir bar, added 9-(4-tert-butylpyridin-2-yl)-2'-(4-phenylpyridin-2-yl)-9H-2,9'-bicarbazole (536 mg, 0.87 mmol, 1.0 eq), K_2PtCl_4 (378 mg, 0.91 mmol, 1.05 eq) and nBu_4NBr (28 mg, 0.087 mmol, 0.1 eq). Then, solvent acetic acid (52 mL) was added under nitrogen atmosphere. The mixture was bubbled with nitrogen for 30 min and then the tube was sealed. The mixture was stirred at room temperature for 20 h and then at 105°C to 115°C in an oil bath for another 3 days, cooled down to ambient temperature and water (104 mL) was added slowly. After stirring at room temperature for 10 min, the precipitate was filtered off and washed with water for three times. Then the solid was dried in air under reduced pressure. The collected solid was purified through column chromatography on silica gel using dichloromethane/hexane (2:1) as eluent to obtain the desired product PtN3N-ptb as a red solid 240 mg in 34% yield. The product (335 mg) was further purified by sublimation in a sublimator with four zone controllers at 290°C, 285°C, 190°C, 150°C, 4.1×10^{-6} Torr to obtain red needle crystals 140 mg in 42% yield. 1H NMR (DMSO- d_6 , 400 MHz): δ 1.27 (s, 9H), 7.19 (t, $J = 7.6$ Hz, 1H), 7.32 (t, $J = 7.6$ Hz, 1H), 7.39 to 7.54 (m, 6H), 7.69 (dd, $J = 6.0, 1.6$ Hz, 1H), 7.83 (d, $J = 7.6$ Hz, 1H), 7.88 (d, $J = 8.0$ Hz, 1H), 7.93 (d, $J = 8.0$ Hz, 1H), 7.95 to 8.00 (m, 5H), 8.10 to 8.14 (m, 3H), 8.37

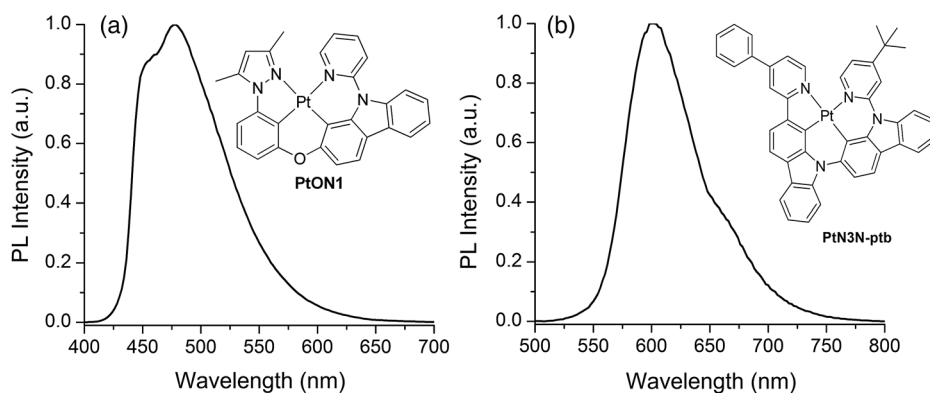


Fig. 1 Room temperature photoluminescent emission spectra of (a) PtON1 and (b) PtN3N-ptb in a dilute solution of CH_2Cl_2 with molecular structures inset.

($d, J = 1.2$ Hz, 1H), 8.55 ($d, J = 6.0$ Hz, 1H), 8.88 ($d, J = 6.4$ Hz, 1H). ^{13}C NMR (DMSO- d_6 , 100 MHz): δ 29.73, 35.51, 111.17, 112.45, 112.87, 113.79, 114.23, 114.98, 115.24, 116.65, 116.97, 117.96, 118.74, 120.40, 120.44, 120.46, 121.56, 121.70, 122.92, 125.30, 126.06, 126.54, 127.27, 127.73, 128.45, 129.36, 130.19, 136.31, 138.03, 138.12, 138.50, 139.65, 143.17, 144.18, 147.72, 149.32, 149.90, 150.51, 163.62, 165.92. MS (MALDI) for $\text{C}_{44}\text{H}_{32}\text{N}_4\text{Pt}[\text{M}]^+$: calcd 811.2, found 811.2. The structure of PtN3N-ptb is given in Fig. 1.

2.3 Device Fabrication and Characterization

Devices were fabricated on glass substrates with previously patterned indium tin oxide (ITO), which formed the anode. Prior to deposition, the substrates were cleaned using a sequence of hand soap scrub then sonication in deionized water, acetone, and isopropyl alcohol. Organic and cathode layers were deposited by vacuum thermal evaporation in a system from Trovato Manufacturing, Victor, New York, and all depositions were done at a pressure less than 5×10^{-7} Torr. Film thicknesses and deposition rates were monitored using a quartz crystal microbalance. Organic materials were deposited at rates from 0.5 to 1.5 Å/s and LiF was deposited at ~ 0.2 Å/s. Al cathodes were deposited at 1 to 2 Å/s through a metal shadow mask, without breaking vacuum, to define device areas of 4 mm^2 in a crossbar structure. The devices were characterized by current–voltage–luminance measurements and electroluminescence (EL) measurements. Current–voltage–luminance data were collected using a Keithley 2400 sourcemeter, Keithley 6485 picoammeter, and Newport 818-UV photodiode. EL data were taken using an Ocean Optics HR4000 spectrometer, Dunedin, Florida. All EL spectra were taken at a current density of 1 mA/cm^2 unless otherwise noted. Electrical characterization was done in a dry nitrogen glovebox before doing the EL measurements in ambient environment.

3 Results and Discussion

3.1 Single-Emitter Devices

Two tetradentate Pt emitters were selected for use in WOLED devices: PtN3N-ptb (red), and PtON1 (blue) due to their complementary emission spectra shown in Fig. 1. Monochrome devices of these emitters were fabricated to determine the current–voltage–luminance and external quantum efficiency (EQE) of each emissive layer. The device structure was as follows: ITO/HAT-CN (10 nm)/NPD (40 nm)/TAPC (10 nm)/emissive layer (EML) (x% emitter:26 mCPy (25 nm)/DPPS (10 nm)/BmPyPB (40 nm)/LiF (1 nm)/Al (100 nm). The blue dopant was PtON1 and the red dopant was PtN3N-ptb. Dopant concentration was 6% PtON1 for the blue in order to optimize the EQE following the previous literature report.²⁰ Red devices, however, were fabricated with dopant concentrations of both 2% PtN3N-ptb and 6% PtN3N-ptb in order to see the effect of dopant concentration on both the EL spectrum and the EQE. Electroluminescent emission (EL) spectra were collected at a current density of 1 mA/cm^2 . The results are summarized in Fig. 2. The blue device demonstrated strong deep blue emission between 450 and 500 nm, similar to previously reported values which should yield appropriate breadth of emission to achieve high color rendering index (CRI).²⁰ Furthermore, the blue device was very efficient with a maximum EQE of 21.2%. The 2% PtN3N-ptb-doped device had λ_{max} at 588 nm but with a sharp drop off in emission intensity beyond 600 nm yielding Commission Internationale de l'Eclairage (CIE) coordinates of (0.57, 0.42). The 6% PtN3N-ptb-doped device was slightly red shifted with λ_{max} at 594 nm and an elevated shoulder around 650 nm yielding slightly improved CIE coordinates (0.59, 0.40). However, this improved color is accompanied by a significant drop in device performance with peak EQE of 15.0% compared with 18.0% for devices with 2% PtN3N-ptb. The reasons for this drop off in efficiency may be related to charge imbalance and triplet–triplet annihilation processes at the higher dopant concentration but will require more study to uncover which factors affect the efficiencies in these red emitting devices.²¹ The high efficiencies of both the blue and red emitters and the complementary nature of their emission spectra make them good candidates in the fabrication of simple two layer white OLEDs employing platinum emitters.

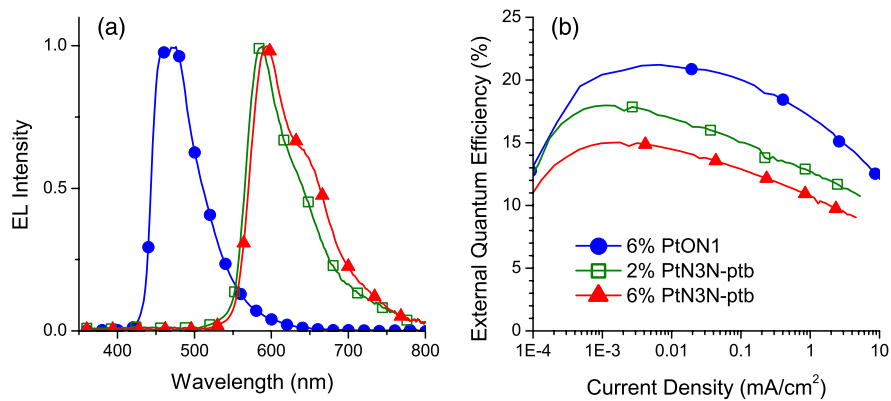


Fig. 2 (a) Electroluminescent spectra at 1 mA/cm² and (b) external quantum efficiency (EQE) versus current density for devices in the structure: ITO/HATCN/NPD/TAPC/EML/DPPS/BmPyPB/LiF/Al, where EML is 25 nm 6% PtON1:26mCPy (circles), 25 nm 2% PtN3N-ptb:26mCPy (squares), or 25 nm 6% PtN3N-ptb:26mCPy (triangles).

3.2 Two-Layer White Devices

There are a large number of strategies for the fabrication of white OLEDs utilizing phosphorescent emitters including: multiple emissive layers, multiple dopants within a single layer, tandem devices, combination of fluorescent, and phosphorescent emissive materials, or single-doped excimer-based white emission.⁶ The most common structure typically employs three separate emissive layers each containing red, green, or blue emissive species since it is easier to achieve the exact specified color by balancing the three emission peaks. However, the fabrication of such a device can prove challenging as modifying the emission spectrum may come with a reduction in efficiency and optimizing the location of the recombination zone may lead to spectral shift at different driving conditions. Thus, as suggested in previous reports, the combination of blue and orange-red emission may be sufficient to optimize a WOLED device for appropriate white color and high efficiency.²² Furthermore, such a simple structure will elucidate the energy transfer and emission processes within the device to give a clear understanding of the optimal device design.

WOLEDs employing two EML layers were made using the blue and red emitters in the structure: ITO/HAT-CN (10 nm)/NPD (40 nm)/TAPC (10 nm)/EML1 (6% emitter: 26 mCPy (x nm)/EML2 (6% emitter: 26 mCPy (y nm)/DPPS (10 nm)/BmPyPB (40 nm)/LiF (1 nm)/Al (100 nm). A doping concentration of 6% was chosen for the red EML, despite the slightly lower EQE than the 2% red device, since the slight red shift and the more pronounced shoulder should produce WOLEDs with higher CRI. Two structures for the white devices were tested in order to explore the nature of exciton formation and energy transfer within the devices: one with an EML composed of a blue emissive layer followed by a red emissive layer, denoted B/R, and another structure with a red emissive layer followed by a blue emissive layer which is denoted as R/B. The blue EML thickness was fixed at 20 nm in each case, whereas the red EML thickness was set at either 2 or 3 nm. The red layer is kept very thin to balance the emission by accounting for favorable energy transfer to the red dopant molecules from other regions of the device as has been reported in the various literature reports.²³ The results are shown in Fig. 3 and a summary of CIE and CRI values as well as efficiency data is presented in Table 1.

The EQE data shown in Fig. 3(b) demonstrates that there is minimal difference between structures with the emissive layer order B/R or R/B with the highest peak quantum efficiency at ~23.1% achieved for the B/R device with an EML 6% PtON1 (20 nm)/6% PtN3N-ptb (2 nm) and the lowest peak EQE of 21.6% for the R/B device with an EML 6% PtN3N-ptb (3 nm)/PtON1 (20 nm). The electroluminescent emission spectra, however, were extremely different depending on the order or the thickness indicating that the high efficiencies are approximately independent of the emission spectrum. In the R/B structure, the blue emission from the PtON1 layer dominates, whereas in the B/R structure, the red emission from the PtN3N-ptb layer dominates. This suggests that the majority of exciton formation is in the region near the hole blocking

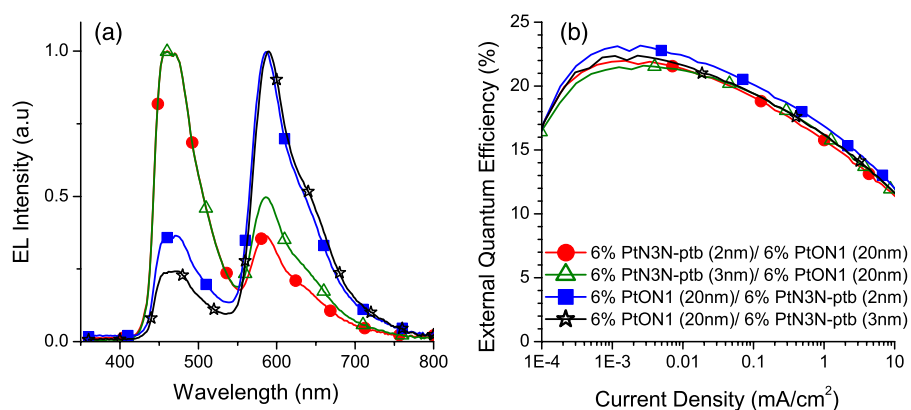


Fig. 3 (a) Electroluminescent spectra at 1 mA/cm² and (b) EQE vs. current density for the devices in the structure: ITO/HATCN/NPD/TAPC/EML/DPPS/BmPyPB/LiF/AL, where EML is 2 nm 6% PtN3N-ptb/20 nm 6% PtON1 (circles), 3 nm 6% PtN3N-ptb/20 nm 6% PtON1 (triangles), 20 nm 6% PtON1/2 nm 6% PtN3N-ptb (squares), or 20 nm 6% PtON1/3 nm 6% PtN3N-ptb (stars).

layer, DPPS. This can be explained by the strong-hole blocking capabilities of DPPS and the strong-hole mobility of the the hole transport and host materials.¹⁸ Nevertheless, a variety of other energy transfer processes are also present in the device which will be described below.

In the R/B device, the majority of excitons are formed within the blue emissive layer at the HBL interface yet some excitons may be formed throughout the EML or could diffuse toward the red emissive layer adjacent to the EBL due to the long triplet diffusion length estimated at up to 100 nm.²⁴ Excitons near the red emissive layer will undergo rapid radiationless energy transfer to the red dopant molecules due to their lower triplet energies, which in turn will emit the red light. This energy transfer process has been reported to occur for distances of <5 nm; thus, the majority of the excitons formed near the HBL interface will not transfer to the PtN3N-ptb emitter since the blue layer is kept sufficiently thick and the blue emission will be dominant.²⁵ The peak intensity in the red portion of the spectrum increased with increasing red EML thickness due to the increase in number of red dopant species for excitons to form on, indicating that there is likely some degree of direct exciton formation within the red layer. As a result, the CIE coordinates shift from (0.25, 0.25) to (0.28, 0.27) and as the thickness of the red EML is increased from 2 to 3 nm and ultimately a CRI of 65 is achieved for the device with a 3 nm 6% PtN3N-ptb/20 nm 6% PtON1 dual emissive layer.

Similarly, in the B/R devices, the majority of the excitons form near the HBL interface. As a result, the red emission is significantly stronger than that of the blue layer, despite the relatively thin red emissive layer of only 2 to 3 nm. Also, as discussed previously, excitons within a few nanometers of this layer have a high probability of energy transfer to the red dopant molecules. Yet, due to the thicker PtON1-doped blue layer, excitons formed beyond the Förster radius of the red EML were able to emit from the PtON1 emitters and thus a small-blue peak is still observed. When decreasing the thickness of the red EML, there was a decrease in the red emission relative

Table 1 CIE and CRI values by device structure.

Structure	CIE ^a	CRI ^a	100 cd/m ²			1000 cd/m ²		
			η_{EQE} (%)	η_A (cd/A)	η_P (lm/W)	η_{EQE} (%)	η_A (cd/A)	η_P (lm/W)
2 nm R/20 nm B	(0.25, 0.25)	—	16.5	29.4	18.5	12.2	22.0	11.0
3 nm R/20 nm B	(0.28, 0.26)	65	18.0	31.6	19.5	13.6	24.0	11.8
20 nm B/2 nm R	(0.45, 0.36)	56	18.8	39.8	25.0	14.5	30.8	15.4
20 nm B/3 nm R	(0.49, 0.37)	50	18.1	36.0	21.7	13.8	27.6	13.0

^aElectroluminescent spectra data collected at 1 mA/cm².

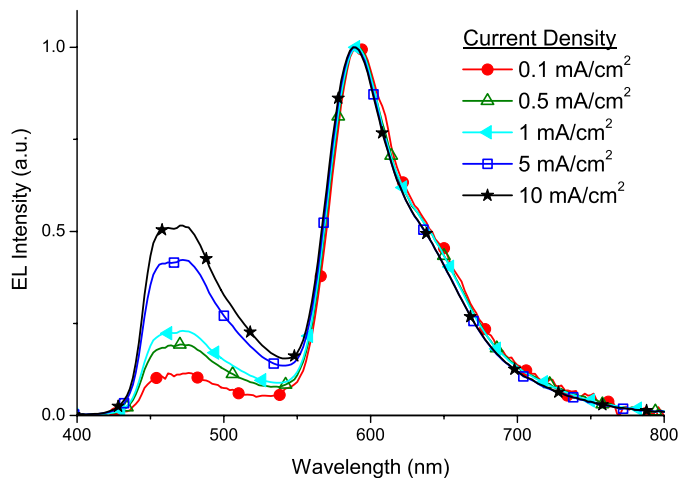


Fig. 4 Electroluminescent spectra versus current density for the device: ITO/HATCN/NPD/TAPC/20 nm 6% PtON1/3 nm 6% PtN3N-ptb/DPPS/BmPyPB/LiF/Al.

to the blue emission as a result of fewer dopant molecules for emission to occur. Also, the peak emission of 586 nm for the device with 2 nm red EML slightly shifted to 590 nm for the device with 3-nm red EML and also showed a more pronounced shoulder.

One major drawback with the multiple emissive layer structure is the relatively poor color stability with changing driving conditions as a result of shifting or spreading the primary recombination zone. As an example, the dependence of the EL spectrum on current density for the device ITO/HATCN (10 nm)/NPD (40 nm)/TAPC (10 nm)/(6% PtON1: 26 mCPy (20 nm))/(6% PtN3N-ptb:26 mCPy (3 nm)/DPPS (10 nm)/BmPyPB (40 nm)/LiF (1 nm)/Al (100 nm) is given in Fig. 4. As the current density increases the ratio of blue to red emission increases by nearly 500%. Consequently, the devices achieve dramatically different emission color within the current range of 0.1 to 10 mA/cm² with CIE coordinates ranging from (0.54,0.39) to (0.45,0.35), respectively. More work is needed to develop better charge transport materials or further optimize device architectures in order to reduce this strong driving condition dependence going forward.

4 Conclusion

We have demonstrated for the first time a WOLED with EQE over 20% can be fabricated using exclusively Pt-based emitters. Two structures were compared by varying the order of the blue and red emitters in the device. EL spectra for devices with the hole transport layer/electron blocking layer/red EML/blue EML/hole blocking layer structure had dominant emission in the blue portion of the spectrum, while the converse was true for devices with the emitter layer order reversed. This confirmed that the majority of exciton generation occurs in the layer closest to the hole blocker layer. A maximum CRI of 65 was achieved with 3-nm red/20-nm blue structure. An improved CRI should be obtainable by adding a suitable green emitter to the device. This work is in progress and will be reported in the near future.

Acknowledgments

The authors thank the National Science Foundation CHE-0748867, Universal Display Corporation, and DOE-EE0005075 for partial support of this work. The Flexible Display Center is sponsored by the Army Research Laboratory (ARL) and was accomplished under Cooperative Agreement 911NG-04-2-005. The views and conclusions contained in this document are those of the authors and should not be interpreted as representing the official policies, either expressed or implied, of the ARL or the U.S. Government. The U.S. Government is

authorized to reproduce and distribute reprints for government purposes, notwithstanding any copyright notation herein.

References

1. C. J. Humphreys, "Solid state lighting," *MRS Bull.* **33**(4), 459–470 (2008), <http://dx.doi.org/10.1557/mrs2008.91>.
2. U.S. Department of Energy, Building Technologies Office, "Solid State Lighting: Brilliant Solutions for America's Energy Future," available at http://apps1.eere.energy.gov/buildings/publications/pdfs/ssl/ssl-overview_brochure_feb2013.pdf (February 2013).
3. S. Pimputkar et al., "Prospects for LED lighting," *Nat. Photonics* **3**(4), 180–182 (2009), <http://dx.doi.org/10.1038/nphoton.2009.32>.
4. A. Panahi, "Challenges and opportunities in LED based lighting," *Proc. SPIE* **8720**, 87200G (2013), <http://dx.doi.org/10.1117/12.2017987>.
5. P. A. Levermore et al., "Phosphorescent organic light-emitting diodes for high-efficacy long-lifetime solid-state lighting," *J. Photon. Energy* **2**(1), 021205 (2012), <http://dx.doi.org/10.1117/1.JPE.2.021205>.
6. M. C. Gather, A. Kohnen, and K. Meerholz, "White organic light-emitting diodes," *Adv. Mater.* **23**(2), 233–248 (2011), <http://dx.doi.org/10.1002/adma.v23.2>; Y.-S. Tyan, "Organic light-emitting-diode lighting overview," *J. Photon. Energy* **1**(1), 011009 (2011), <http://dx.doi.org/10.1117/1.3529412>.
7. S. Reineke et al., "White organic light-emitting diodes with fluorescent tube efficiency," *Nature* **459**, 234–239 (2009), <http://dx.doi.org/10.1038/nature08003>.
8. L. Xiao et al., "Recent progresses on materials for electrophosphorescent organic light-emitting devices," *Adv. Mater.* **23**(8), 926–952 (2011), <http://dx.doi.org/10.1002/adma.v23.8>.
9. M. A. Baldo et al., "Highly efficient phosphorescent emission from organic electroluminescent devices," *Nature* **395**(6698), 151–154 (1998), <http://dx.doi.org/10.1038/25954>.
10. H. Yersin and W. J. Finkenzeller, "Triplet emitters for organic light - emitting diodes: basic properties," *Highly Efficient OLEDs with Phosphorescent Materials*, H. Yersin, Ed., p. 35, Wiley-VCH Verlag GmbH & Co. KGaA, Weinheim (2008).
11. Y. Sun and S. R. Forrest, "High-efficiency white organic light emitting devices with three separate phosphorescent emission layers," *Appl. Phys. Lett.* **91**(26), 263503 (2007), <http://dx.doi.org/10.1063/1.2827178>.
12. S. Lamansky et al., "Synthesis and characterization of phosphorescent cyclometalated iridium complexes," *Inorg. Chem.* **40**(7), 1704–1711 (2001), <http://dx.doi.org/10.1021/ic0008969>.
13. E. Turner, N. Bakken, and J. Li, "Cyclometalated platinum complexes with luminescent quantum yields approaching 100%," *Inorg. Chem.* **52**(13), 7344–7351 (2013), <http://dx.doi.org/10.1021/ic302490c>.
14. J. A. Gareth Williams et al., "Optimizing the luminescence of platinum(II) complexes and their applications in organic light-emitting devices (OLEDs)," *Coord. Chem. Rev.* **252**(23–24), 2596–2611 (2008), <http://dx.doi.org/10.1016/j.ccr.2008.03.014>.
15. B.-P. Yan et al., "Efficient white organic light-emitting devices based on phosphorescent platinum(II)/fluorescent dual-emitting layers," *Adv. Mater.* **19**(21), 3599–3603 (2007), [http://dx.doi.org/10.1002/\(ISSN\)1521-4095](http://dx.doi.org/10.1002/(ISSN)1521-4095).
16. N. Chopra et al., "High efficiency and low roll-off blue phosphorescent organic light-emitting devices using mixed host architecture," *Appl. Phys. Lett.* **97**(3), 033304 (2010), <http://dx.doi.org/10.1063/1.3464969>.
17. E. L. Williams et al., "Excimer-based white phosphorescent organic light-emitting diodes with nearly 100% internal quantum efficiency," *Adv. Mater.* **19**(2), 197–202 (2007), [http://dx.doi.org/10.1002/\(ISSN\)1521-4095](http://dx.doi.org/10.1002/(ISSN)1521-4095).
18. L. Xiao et al., "Nearly 100% internal quantum efficiency in an organic blue-light electrophosphorescent device using a weak electron transporting material with a wide energy gap," *Adv. Mater.* **21**(12), 1271–1274 (2009), <http://dx.doi.org/10.1002/adma.v21:12>.
19. H. Sasabe et al., "Wide-energy-gap electron-transport materials containing 3,5-dipyridyl-phenyl moieties for an ultra high efficiency blue organic light-emitting device," *Chem. Mater.* **20**(19), 5951–5953 (2008), <http://dx.doi.org/10.1021/cm801727d>.

20. X. Hang et al., "Highly efficient blue-emitting cyclometalated platinum(II) complexes by judicious molecular design," *Angew. Chem. Int. Ed.* **52**(26), 6753–6756 (2013), <http://dx.doi.org/10.1002/anie.v52.26>.
21. C.-L. Ho et al., "Red-light-emitting iridium complexes with hole-transporting 9-arylcarbazole moieties for electrophosphorescence efficiency/color purity trade-off optimization," *Adv. Funct. Mater.* **18**(2), 319–331 (2008), [http://dx.doi.org/10.1002/\(ISSN\)1616-3028](http://dx.doi.org/10.1002/(ISSN)1616-3028).
22. R. Wang et al., "Highly efficient orange and white organic light-emitting diodes based on new orange iridium complexes," *Adv. Mater.* **23**, 2823–2827 (2011), <http://dx.doi.org/10.1002/adma.201100302>.
23. B.W. D'Andrade and S. R. Forrest, "White organic light-emitting devices for solid-state lighting," *Adv. Mater.* **16**(18), 1585–1595 (2004), [http://dx.doi.org/10.1002/\(ISSN\)1521-4095](http://dx.doi.org/10.1002/(ISSN)1521-4095).
24. B. W. D'Andrade, M. E. Thompson, and S. R. Forrest, "Controlling exciton diffusion in multilayer white phosphorescent organic light emitting devices," *Adv. Mater.* **14**(2), 147–151 (2002), [http://dx.doi.org/10.1002/\(ISSN\)1521-4095](http://dx.doi.org/10.1002/(ISSN)1521-4095).
25. R. S. Deshpande, V. Bulovic, and S. R. Forrest, "White-light-emitting organic electroluminescent devices based on interlayer sequential energy transfer," *Appl. Phys. Lett.* **75**(7), 888–890 (1999), <http://dx.doi.org/10.1063/1.124250>.

Barry P. O'Brien is a principal process engineer at the Arizona State University Flexible Display Center, where he works on thin film process development, characterization, and organic light-emitting diode devices. He has 12 publications, one issued patent, and two patents pending. His research interests include organic and inorganic electronics, thin-film processing, materials characterization, and device fabrication. He is pursuing his PhD degree in materials science and engineering at Arizona State University.

Biographies of the other authors are not available.